

Features of structuring and ablation of thin titanium films by femtosecond laser pulses

© E.V. Kuzmin, A.V. Klekovkin

Lebedev Physical Institute, Russian Academy of Sciences, Moscow, Russia

e-mail: kuzmin_evg@live.ru

Received December 20, 2021

Revised December 20, 2021

Accepted December 30, 2021

The processes of structuring and ablation of a titanium film by femtosecond laser pulses at wavelengths of 515 nm and 1030 nm have been studied in both single-pulse and multi-pulse modes. The optimal energy regimes for the selective removal of film material without damaging the substrate, as well as the regimes for the generation of the periodic structures on the surface, are determined. The evolution of periodic structures with an increase in the number of laser pulses is shown. The precision removal of titanium film is associated with thermomechanical explosive boiling and the corresponding energy contribution, which ensures the cascade appearance of ablation craters.

Keywords: thin films, femtosecond laser pulses, surface treatment

DOI: 10.21883/EOS.2022.04.53727.66-21

Introduction

Titanium is a widespread structural material. Currently, in order to enhance its performance advantages, nanostructuring and surface microprocessing by laser pulses with various lengths are widely used [1]. More frequently these processes involve laser ablation [2] which has several implementation mechanisms depending on the energy expended for the material. One of such mechanisms is spallation ablation caused by the presence of strong compressive stresses in the subsurface layer which are caused by the difference in laser heating time and the time required for material expansion [3,4]. As a result of spallation ablation, ablation craters of a typical shape (distinct boundary and flat bottom) appear on the target surface, and the crater depth does not depend on the expended energy, while, when the phase explosion threshold is achieved, the crater depth grows quickly with the increase in the emission energy density. The spallation ablation together with surface structuring have a special place in multilayer film technologies. One of the unique capabilities of such processes is a selective action on only the upper layer of a multilayer specimen without damaging the underlying layers [5,6], however, the search for optimum gentle action conditions is still under way.

The research is focused on thin titanium films on silicon substrates investigated at various energies in pulse (E), wavelengths (λ) and number of pulses (N). Silicon as the basic material in microelectronics is highly demanded nowadays and the ability to control Ti/Si film topology opens new perspectives for fictionalization of various surfaces. After the exposure, the specimens were examined by scanning electron microscopy (SEM) and energy-dispersive X-ray spectroscopy (EDX) methods.

Thin titanium films (30 nm) produced by magnetron sputtering with high-purity Ti evaporation onto silicon substrates (Si(100), $h = 0.5$ mm) were used as specimens.

Experimental

The specimen surface was processed with focused laser beam in air in normal exposure conditions. Satsuma (Amplitude Systems) optical fiber laser generating linearly polarized emission with a wavelength of 515 and 1030 nm, pulse lengths of 300 fs and varied pulse repetition rate up to 100 kHz was used as an ultrashort laser pulse source. Laser emission with Gaussian intensity distribution was directed into the microscope and focused on the specimen

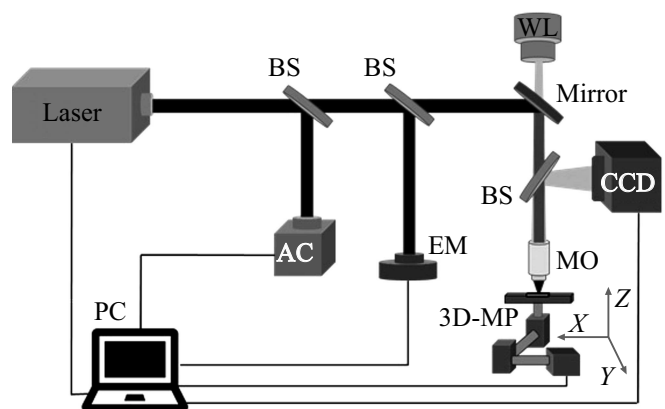


Figure 1. Fs/ps-laser ablation workstation setup: BS — beamsplitter, EM — energy meter, AC — autocorrelator, MO — microscope objective lens, WL — white-light source, PC — computer with preinstalled dedicated laser, camera, positioning system control software, CCD — camera for surface visualization during scanning.

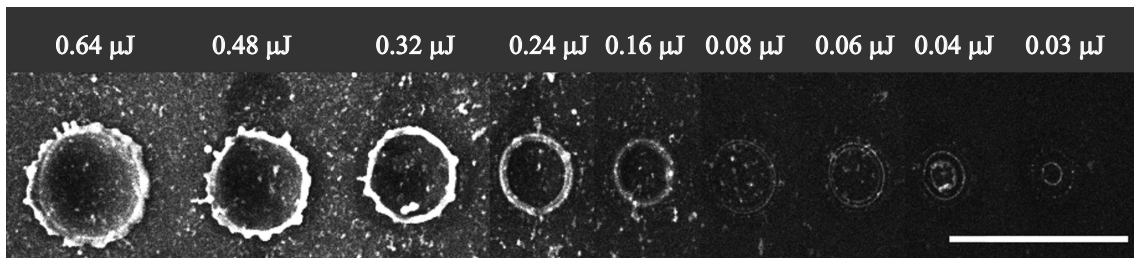


Figure 2. SEM image of single-pulse craters obtained at various energies $\lambda = 515$ nm. Scale bar corresponds to $10 \mu\text{m}$.

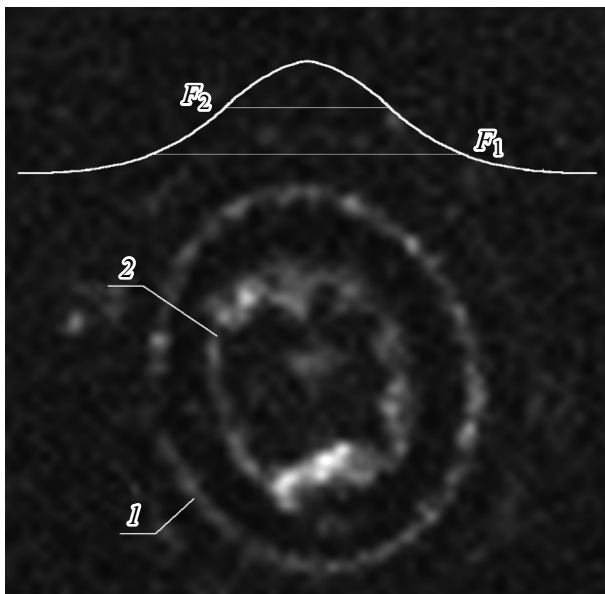


Figure 3. magnified image of a single-pulse crater for energy $0.04 \mu\text{J}$. 1 — spallation ablation crater boundary; 2 — molten region boundary; white line shows the laser pulse shape. F_1 — spallation ablation threshold, F_2 — melting threshold.

using the microscope objective ($NA = 0.25$), and the focal spot at $1/e$ was equal to $2.2 \pm 0.2 \mu\text{m}$ (515 nm) and $2.8 \pm 0.2 \mu\text{m}$ (1030 nm). The maximum pulse energy was equal to $0.64 \mu\text{J}$ (515 nm) and $3.3 \mu\text{J}$ (1030 nm), and the maximum energy density corresponding to them was equal to 3.36 and 10.09 J/cm^2 .

Experimental setup used for laser ablation is shown in Fig. 1.

A three-axis movable platform with a minimum increment 150 nm and movement velocity up to $200 \mu\text{m/s}$ was used to secure the specimen and, thus, to implement the single-pulse ablation mode (each pulse to new point) with continuous specimen movement.

Two film exposure modes were used. The first mode involved single-pulse ablation with pulse energy variation, and the second mode involved variation of not only the pulse energy, but also the number of pulses (from 1 to 100), which enabled to define optimum modes for generation of periodic surface structures (PSS).

Results and discussion

Fig. 2 shows SEM images of craters on the titanium film surface obtained in the single-pulse mode with exposure at 515 nm. It can be seen that when the expended energy grows, not only the ablation crater size, but also appearance are changed which proves that various ablation mechanisms are implemented.

Thus, the spallation ablation mode (0.03 – $0.08 \mu\text{J}$) is the most low-energy mode among the observed surface modification modes. In such mode (Fig. 3), the laser pulse energy in the focal spot center exceeds the material melting threshold which results in the formation of a crater with a surrounding re-solidified material ring. In addition, the same pulse energy on the focal spot edges is insufficient for melting, but exceeds the spallation ablation threshold which is expressed in the emergence of a crater with flat bottom around the molten region [7].

Increase in the pulse energy (0.16 – $0.32 \mu\text{J}$) results in growth of the spallation ablation crater diameter, however, „residual“ laser pulse energy also increases due to which the size of the molten „internal“ zone grows and then two crater boundaries merge, and the higher the expended energy is,

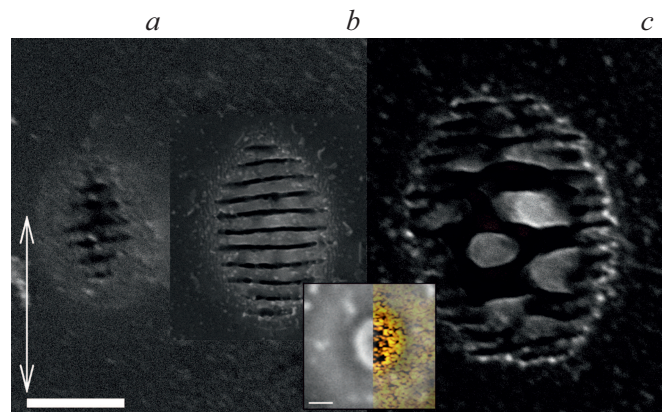


Figure 4. SEM image of multipulse craters. $\lambda = 515$ nm. Pulse repetition rate is 5 Hz. Scale bar corresponds to $2 \mu\text{m}$, the arrow shows the emission polarization. Pulse energy $0.02 \mu\text{J}$ — 50 pulses (a), $0.02 \mu\text{J}$ — 100 pulses (b), $0.03 \mu\text{J}$ — 100 pulses (c). Detail — combined SEM/EDX image of surface structures obtained at $0.02 \mu\text{J}$ and 100 pulses. Scale bar corresponds to $2 \mu\text{m}$. Yellow dots denote titanium particles.

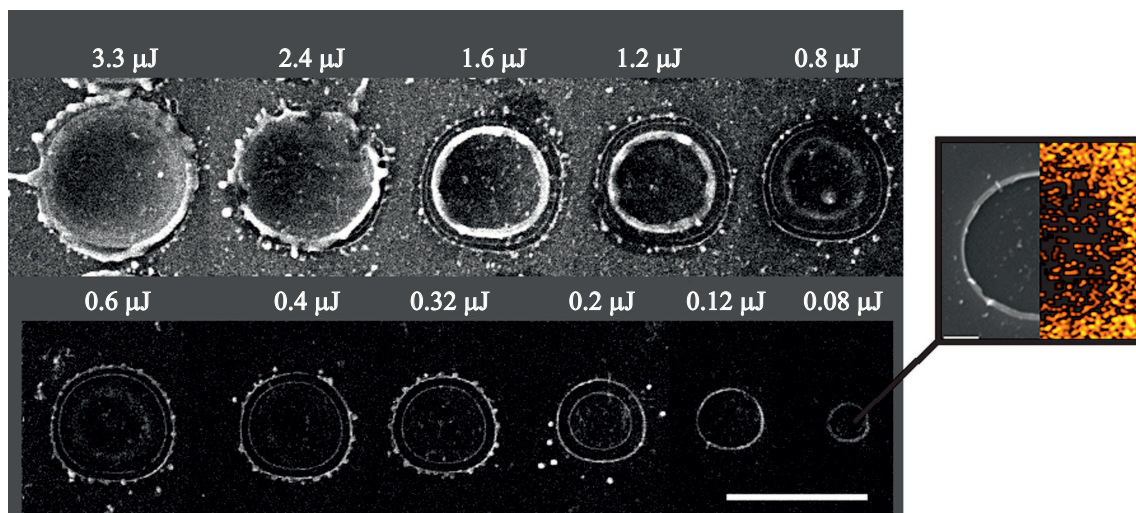


Figure 5. SEM image of single-pulse craters obtained at various energies and at 1030 nm. Scale bar corresponds to $10\ \mu\text{m}$. Detail: combined SEM/EDX image of single-pulse crater obtained at $0.08\ \mu\text{J}$. Scale bar corresponds to $2\ \mu\text{m}$. Yellow dots denote titanium particles.

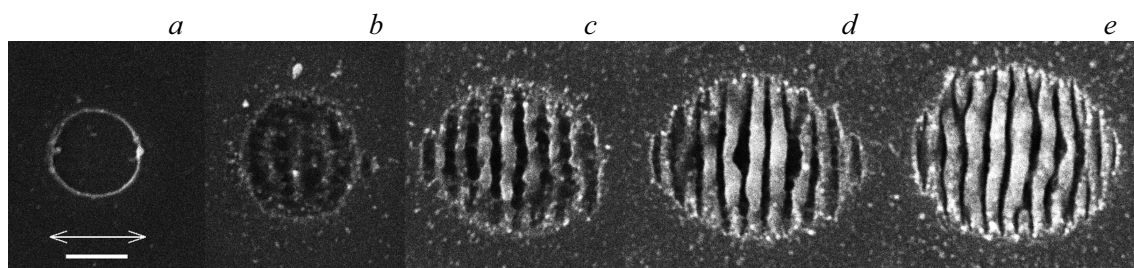


Figure 6. SEM image of multipulse craters 1030 nm. Pulse repetition rate is 5 Hz. Scale bar corresponds to $2\ \mu\text{m}$, the arrow shows the emission polarization. Pulse energy $0.08\ \mu\text{J}$ — 1 pulse (a), $0.08\ \mu\text{J}$ — 10 pulse (b), $0.08\ \mu\text{J}$ — 30 pulses (c), $0.08\ \mu\text{J}$ — 50 pulses (d), $0.08\ \mu\text{J}$ — 100 pulses (e).

the more coarse the re-solidified material ring shape is. At the maximum pulse energy ($0.48\text{--}0.64\ \mu\text{J}$) in the crater center, a molten bath appear which forms a „lens“ upon completion of thermal processes.

In case of multipulse exposure, PSS are formed on the film surface with more successful generation taking place at low energies and large number of pulses.

Thus, during exposure to 50 pulses with energy $0.02\ \mu\text{J}$ (Fig. 4, a), surface structures begin to form with a period $\Lambda \sim 0.36\ \mu\text{m}$ in the exposure zone center (where the energy is maximum). When the number of pulses grows (Fig. 4, b), the generation conditions become more favourable (the structures formed before serve as seed structures) and the PSS formation order is improved. In this case the individual pulse energy does not exceed the spallation ablation threshold and surface wave excitation and, thus, PSS formation take place directly in the thin film which is proved by the presence of periodic titanium traces in the crater center which can be detected using EDX (detail in Fig. 4).

Further increase in the energy/number of pulses results in significant exceedance of the surface structure generation

threshold in the crater center which is expressed in demolition of the ordered structures and formation of molten areas, while PSS generation is continued on the crater edges (Fig. 4, c).

When the specimen is exposed to emission at 1030 nm, the acting ablation mechanisms remain unchanged, however, energy modes are shifted a little. Fig. 5 shows that the spallation ablation mode is observed for energies 0.08 and $0.12\ \mu\text{J}$, while the crater inside surface remains smooth since the „excess“ energy is insufficient for the material to melt. Detail in Fig. 5 shows that in the area, where the spallation ablation occurred, a titanium layer removal is observed (minimum number of residual particles can be explained by dispersion of the ablating material from the adjacent craters). With the energy growth (from 0.2 to $3.2\ \mu\text{J}$), the material melting threshold is exceeded and an „internal“ crater is formed, in the center of which beginning from $0.6\ \mu\text{J}$ a re-solidified molten silicon zone surrounded with a ring is seen in its turn. Thus, for energies 1.2 and $1.6\ \mu\text{J}$, ablation craters have a three-stage appearance which is changed up to a „lens-like“ appearance with further

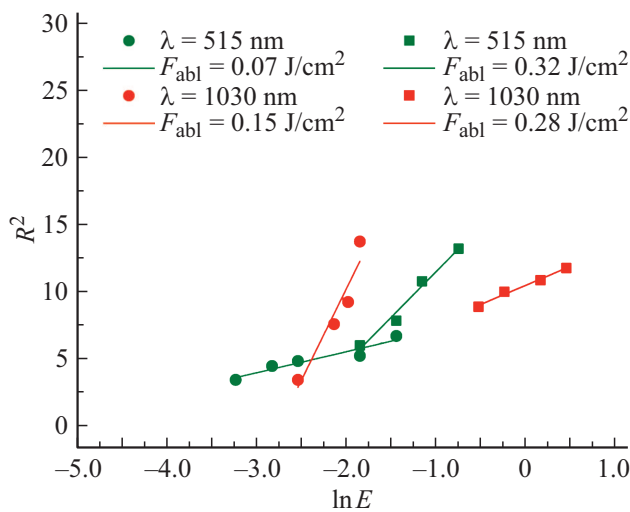


Figure 7. Squared ablation region radius vs. pulse energy logarithm. Spallation ablation craters are shown with circles, ablation craters at phase explosion are shown by squares.

energy growth similar to the craters obtained for high energies at 515 nm.

In case of multipulse exposure (Fig. 6), consequential evolution of ablation craters can be seen according to the increase in the expended energy, however, as opposed to the craters in Fig. 4, the spallation ablation mechanism is implemented as early as in the first pulse due to which the film is removed completely and hence with the next pulses surface waves are excited in substrate and silicon PSS are formed ($\Lambda \sim 0.86 \mu\text{m}$). Further increase in the energy/number of pulses also results in the demolition of structures in the crater center (similar to Fig. 4, c).

Based on the measured sizes of the exposed regions (Fig. 7), curves of squared ablation crater width R_{abl}^2 vs. energy logarithm $\ln E$ were plotted for both wavelengths, as a result of which typical focal spot sizes and modification thresholds were defined [8]. The spallation ablation was characterized by the outside diameters of the corresponding craters and the experimental thresholds were equal to 0.07 ± 0.01 and $0.15 \pm 0.04 \text{ J/cm}^2$ (515 and 1030 nm) which matches with the spallation ablation that had been observed before on bulk titanium and occurred at 0.08 J/cm^2 ($\lambda = 800 \text{ nm}$) [9]. In order to estimate the phase explosion threshold, solidified molten ring diameters were measured for the craters formed at high pulse energies. The threshold energies are equal to $0.32 \pm 0.03 \text{ J/cm}^2$ (515 nm) and $0.28 \pm 0.02 \text{ J/cm}^2$ (1030 nm) and are close to the ablation thresholds for bulk titanium $\sim 0.3 \text{ J/cm}^2$ ($\lambda = 800 \text{ nm}$) [10].

Conclusion

The experiment with titanium film exposure to 300 fs laser pulses at 515 and 1030 nm in single-pulse and multipulse modes enabled to define laser processing conditions in which both selective removal of titanium film without

substrate damage and PSS generation in the film are implemented. The spallation ablation energy thresholds ($0.07 \pm 0.01 \text{ J/cm}^2$ for 515 nm and $0.15 \pm 0.04 \text{ J/cm}^2$ for 1030 nm) and phase explosion thresholds were calculated. These thresholds were close to that of bulk titanium ($0.32 \pm 0.03 \text{ J/cm}^2$ for 515 nm and $0.28 \pm 0.02 \text{ J/cm}^2$ for 1030 nm).

Funding

The authors are grateful to the Russian Science Foundation for the financial support of these research within project 21-79-30063.

Conflict of interest

The authors declare that they have no conflict of interest.

References

- [1] K.C. Phillips, H.H. Gandhi, E. Mazur, S.K. Sundram. *Advances in Optics and Photonics*, **7**(4), 684 (2015). DOI: 10.1364/AOP.7.000684
- [2] A.A. Ionin, S.I. Kudryashov, S.V. Makarov, A.O. Levchenko, A.A. Rudenko, I.N. Saraeva, D.A. Zayarny, C.R. Nathala, W. Husinsky. *Laser Phys. Lett.*, **13**, 025603 (2016). DOI: 10.1088/1612-2011/13/2/025603
- [3] Y.V. Petrov, V.A. Khokhlov, V.V. Zhakhovsky, N.A. Inogamov. *Appl. Surf. Sci.*, **492**, 285–297 (2019). DOI: 10.1016/j.apsusc.2019.05.325
- [4] M.V. Shugaev, L.V. Zhigilei. *Comput. Mater. Sci.*, **166**, 311–317 (2019). DOI: 10.1016/j.commatsci.2019.05.017
- [5] S. Petrovic, B. Salatic, D. Perusko, I. Bogdanovic-Radovic, M. Cekada, B. Gakovic, D. Pantelic, M. Trtica, B. Jelenkovic. *Laser Phys.*, **23**, 026004 (2013). DOI: 10.1088/1054-660X/23/2/026004
- [6] B. Gakovic, P.A. Danilov, S.I. Kudryashov, D. Milovanovic, A. Radulovic, P. Panjan, A.A. Ionin. *Eur. Phys. J. D.*, **75**, 288 (2021). DOI: 10.1140/epjd/s10053-021-00292-4
- [7] C. Wu, L.V. Zhigilei. *Appl. Phys. A*, **1**(114), 11 (2014). DOI: 10.1007/s00339-013-8086-4
- [8] J.M. Liu. *Optics Lett.*, **7**(5), 196 (1982). DOI: 10.1364/OL.7.000196
- [9] C. Nathala, A. Ajami, A.A. Ionin, S.I. Kudryashov, S.V. Makarov, T. Ganz, A. Assion, W. Husinsky. *Opt. Express*, **23**, 5915 (2015). DOI: 10.1364/OE.23.005915
- [10] M. Ye, C.P. Grigoropoulos. *J. Appl. Phys.*, **89**(9), 5183–5190 (2001). DOI: 10.1063/1.1360696